

Supplementary information

Chemically functionalized cellulose triboelectret nanogenerator for machine-learning enabled tactile sensing

Sunidhi Mishra,¹ Dalip Saini,² Sudip Naskar,² Sourav Ghosh,¹ Bidya Mondal,² Dipankar Mandal*,² and Pradip K. Maji*¹

¹Department of Polymer and Process Engineering, Indian Institute of Technology Roorkee, Saharanpur Campus, Saharanpur, 247001, Uttar Pradesh, India

² Quantum Materials and Devices Unit, Institute of Nano Science and Technology, Knowledge City, Sector 81, Mohali 140306, Punjab, India

*Corresponding authors: **Pradip K. Maji**, Email: pradip@pe.iitr.ac.in

Dipankar Mandal, Email: dmandal@inst.ac.in

Experimental details

Materials and reagents

Waste mango wood was obtained from a local field. Ethanol (99.9%) was purchased from Changshu Hongsheng Fine Chemical Co., Ltd. Toluene, sodium sulfite, sodium chlorite, glacial acetic acid, potassium hydroxide, polyvinyl alcohol (PVA, Mw: 145,000 g/mol), acetonitrile, n-hexane, triethylamine, ethyl acetate, nitric acid (68%), and sulfuric acid (95–98%) were purchased from Himedia Pvt. Ltd., India. Stearoyl chloride (purity < 96%) was purchased from TCI Japan. Aluminium tape, double-sided tape, and copper wire were bought from a local provider. Distilled (DI) water was utilized to prepare all aqueous suspensions, and DI water was obtained from laboratory distillation machine. All reagents were utilized as specified without any further processing.

Preparation of cellulose based samples

Extraction of cellulose nanofiber (CNF)

CNF was extracted from waste mango wood by a sequential purification and fibrillation technique. Initially, scrap mango wood was cleaned, sun-dried, and smashed into a fine powder, followed by screening through a 30-mesh screen. Ethanol: toluene (1:2, v/v) mixture was employed for 7-8 hours to remove wax content via Soxhlet extraction. The resulting residue was thoroughly washed with DI water and dried at 50-60 °C overnight. The dried biomass was mixed with a sodium chlorite (NaClO_2) solution of 5 weight percent (%) at pH 4, adjusted with glacial acetic acid to carry out delignification procedure under continuous stirring at 80 °C for 5 hours. The cellulose-chlorite complex was vacuum filtered, fully rinsed with DI water, and subjected to multiple bleaching cycles to ensure complete elimination of lignin. Furthermore, delignified material undergo further treatment using 2 weight percent (%) sodium sulfite (Na_2SO_3) solution about 75 °C for 2 hours to enhance cellulose purity. The processed cellulose was extracted employing vacuum filtering, cleansed with DI water. In addition to remove hemicellulose, 7 weight percent (%) potassium hydroxide (KOH) solution was utilized at 85 °C for 4 hours. The insoluble fraction was removed, washed until a neutral pH was obtained, and subsequently dried in a hot-air oven at 50 °C, providing chemically purified cellulose (CPC).

To make sure uniform dispersion, the CPC solution was undergone to mechanical treatment via a high-speed Ultra-Turrax homogenizer (IKA T25) at 9,000 rpm over 35 min. Nano

fibrillation was carried out via a high-intensity ultra sonicator (SKL-650D, Ningbo Sjia Lab Equipment Co, Ltd, China) operated at 600 W and 20 kHz for 30 min. To reduce excessive heating, the process was performed in an ice bath, keeping the temperature around 25 °C. Milk consistency White cellulose solution turned into thick gel like suspension upon 30 min of ultrasonication, owing to increase in surface area of CNF. The resultant CNF aqueous suspension was stored at 4 °C for further characterization and applications.

Preparation of CNF/PVA composite aerogels

A 5-weight percent (%) PVA solution was prepared by dissolving 5 g of PVA in 100 mL of DI water under continuous stirring at room temperature overnight. PCA were synthesized utilizing a one-pot technique. A homogeneous CNF/PVA suspension was produced by mixing 20 g of 1 weight percent (%) CNF dispersion with PVA solution under continuous stirring for 15 min. Ultrasonication for 15 min enhanced the development of physically cross-linked CNF/PVA hydrogels via hydrogen bonding. The hydrogel was placed into polypropylene molds, frozen at -40 °C for 6 hours, and afterwards freeze-dried at -50 °C for 48 hours (Operon, South Korea) to produce PCA.

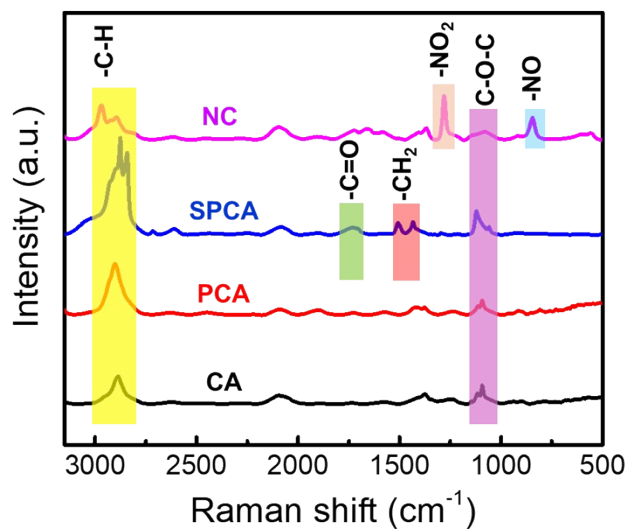


Fig. S1. Raman spectra of CA, PCA, SPCA, and NC film.

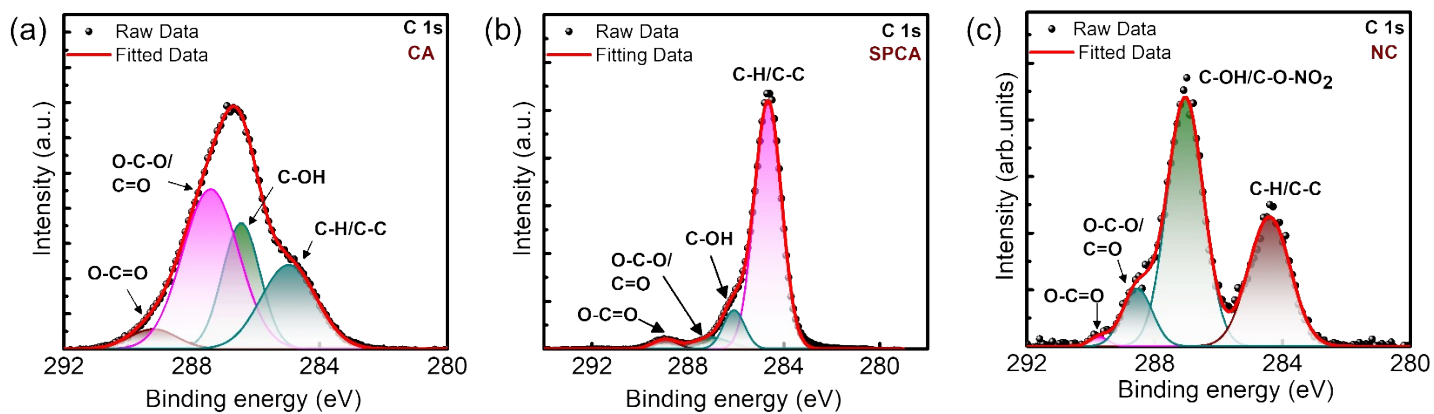


Fig. S2 (a-c) High resolution XPS spectra of C1s for (a) CA, (b) SPCA and (c) NC.

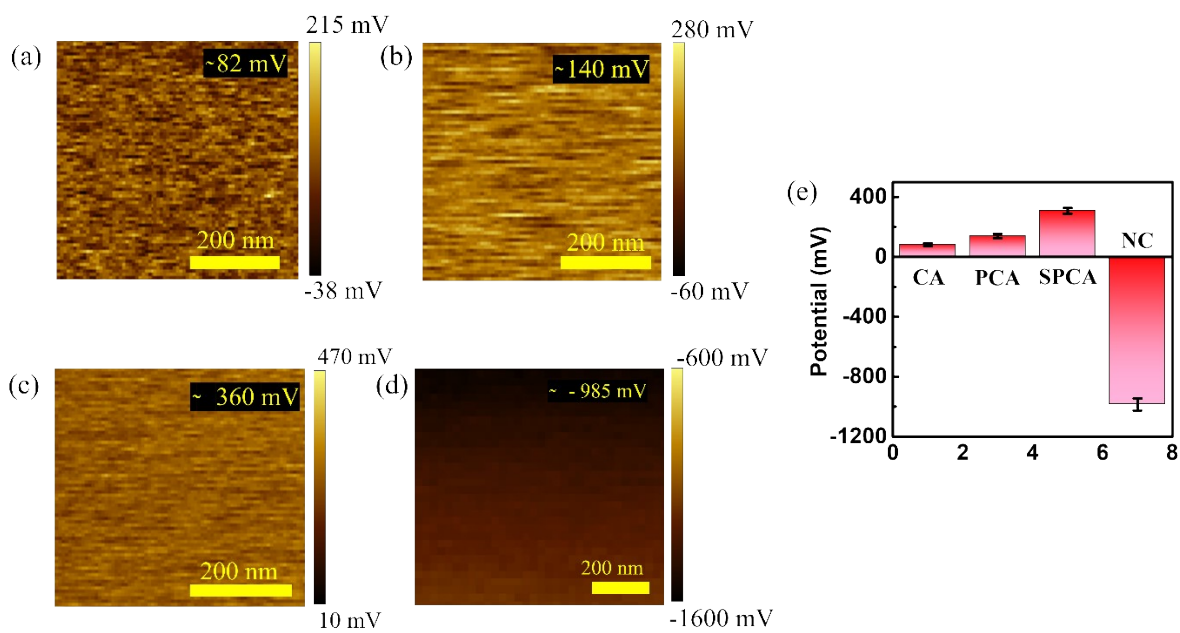


Fig. S3 KPFM potential images of (a-d) (a) CA, (b) PCA, (c) SPCA and (d) NC. (e) Histogram showing average surface potential of CA, PCA, SPCA and NC.

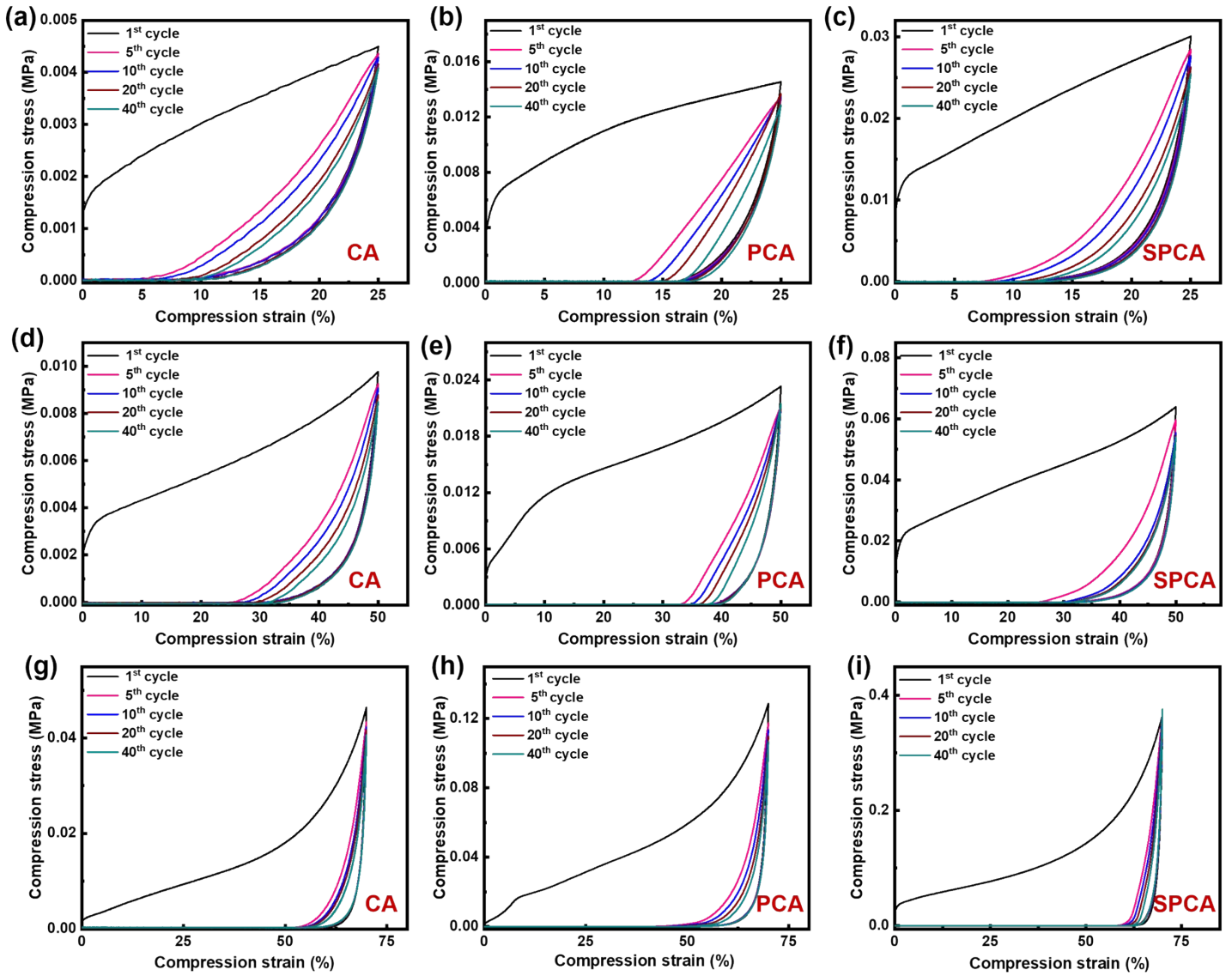


Fig. S4. Cyclic compressive stress-strain curve of CA, PCA, and SPCA at (a-c) 25%, (d-f) 50%, and (g-i) 70%, respectively.

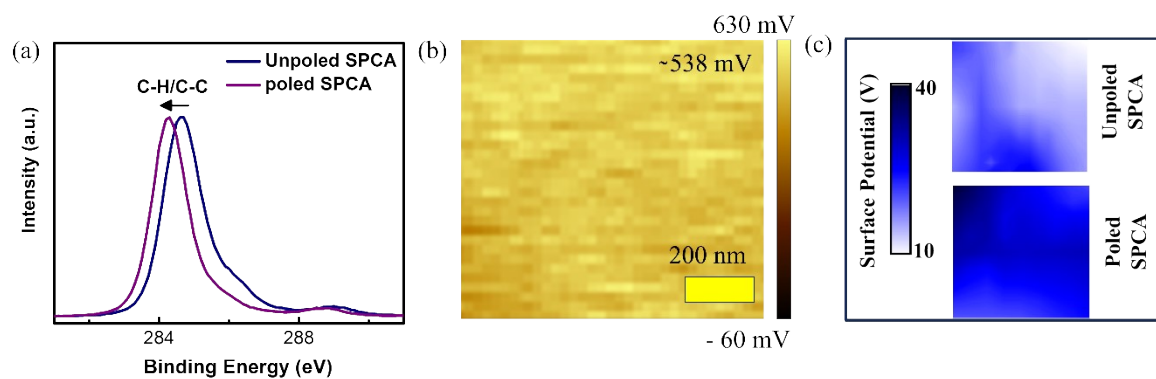


Fig. S5 (a) KPFM surface potential image of poled SPCA. (b) Surface potential mapping of poled and unpoled SPCA. (c) High resolution XPS spectra of C1s for unpoled and poled SPCA.

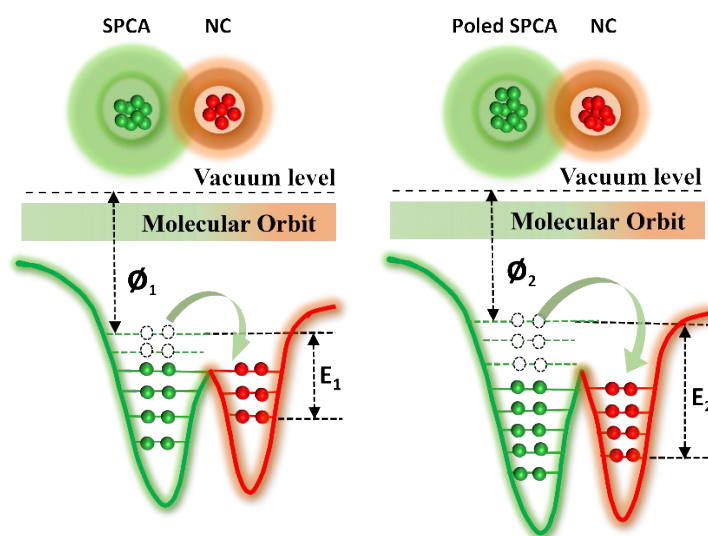


Fig. S6 The electron tunnelling model before and after corona discharge of SPCA.

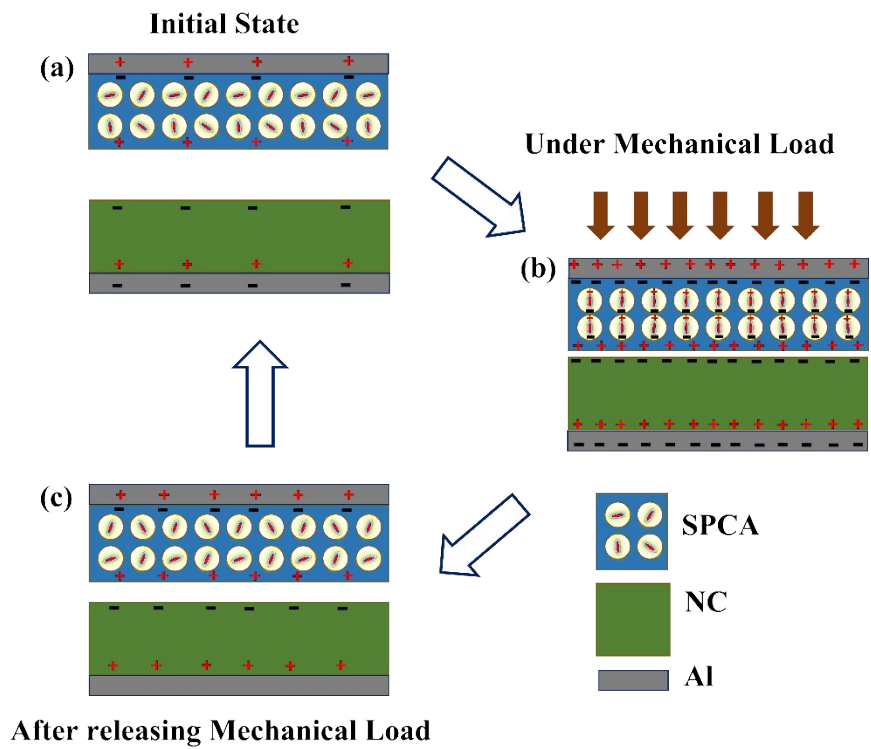


Fig. S7 The charge transfer mechanism of E-TENG is schematically depicted in (a) the starting (and final) state and (b) to (c), demonstrates multiple states that result from applying and release of an external force.

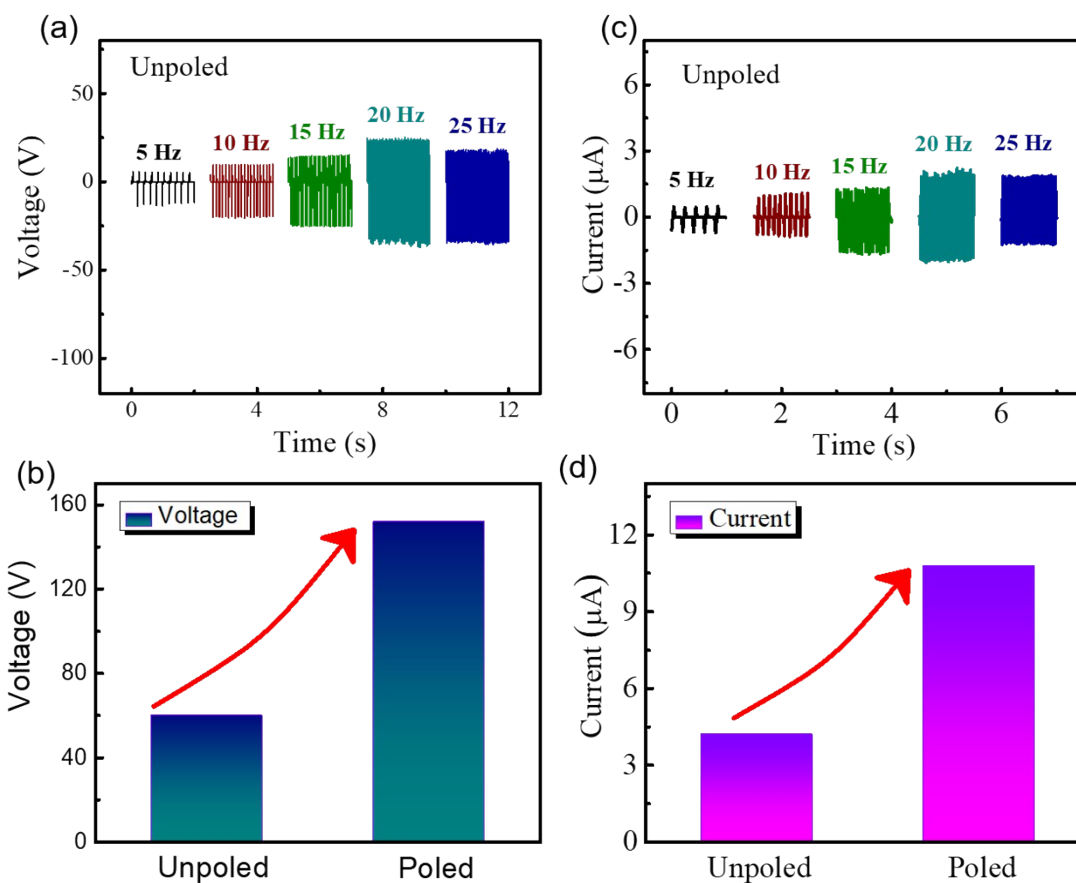


Fig. S8 Electrical output comparison of unpoled and corona-poled E-TENG. (a) V_{oc} and (b) I_{sc} of the unpoled E-TENG at 5-25 Hz. (c, d) Bar charts comparing maximum V_{oc} (~ 50 V vs. ~ 152 V) and I_{sc} (~ 4 μA vs. ~ 10.8 μA) of unpoled and poled E-TENG at 20 Hz.

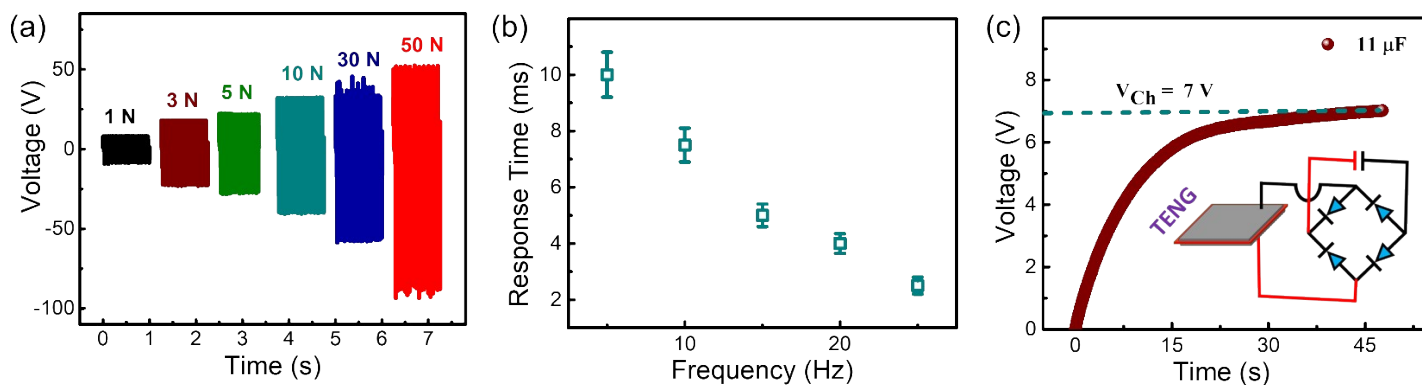


Fig. S9 (a) V_{oc} measured at different applying forces, (b) Response time measured at different frequencies, (c) Capacitor charging performance.

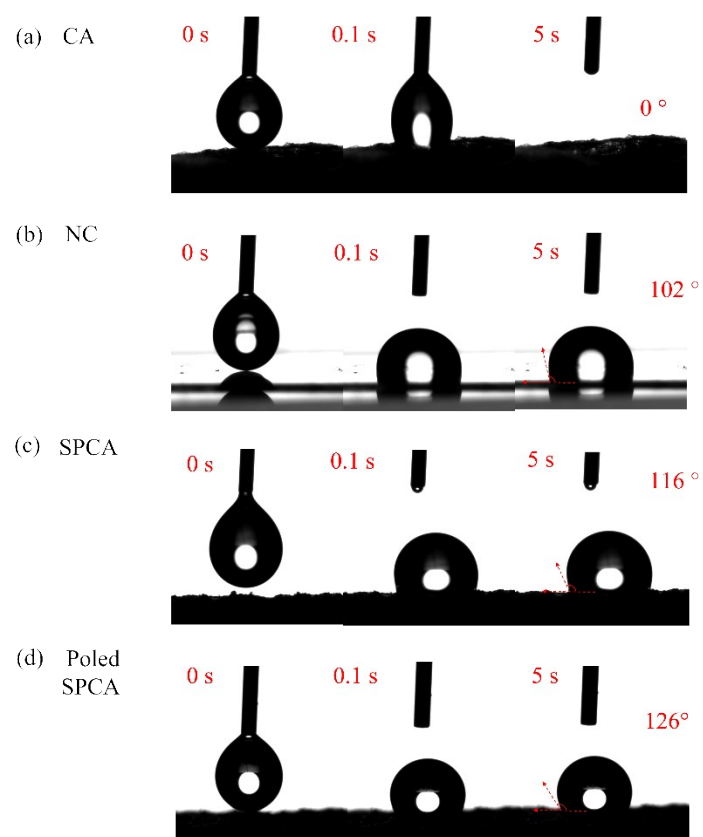


Fig. S10 Water contact angle measurement at 0s, 0.1s and 5s for (a) CA, (b) NC, (c) SPCA, and (d) poled SPCA.

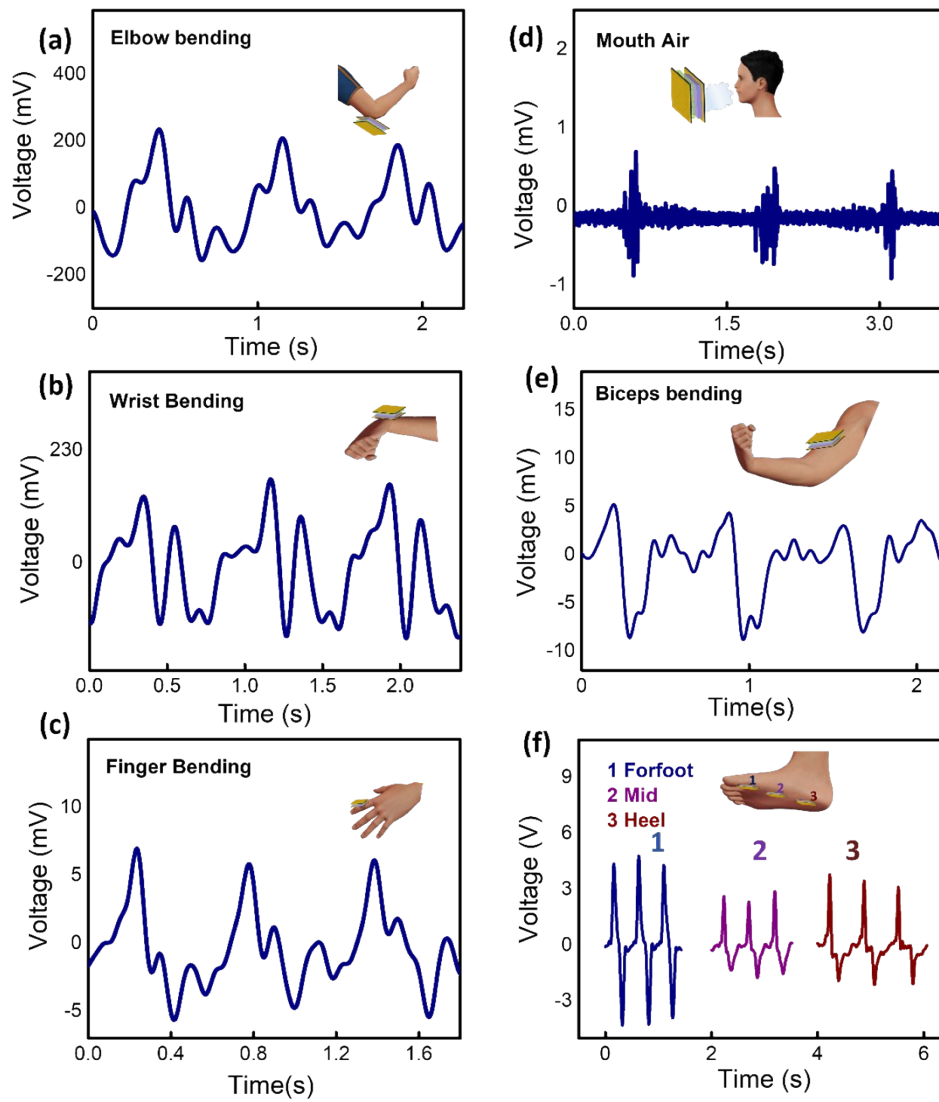


Fig. S11 Human physiological signal health monitoring using E-TENG. (a, b, c and e) Signal monitoring of elbow, wrist, finger and biceps bending respectively. (d) Monitoring of coughing action. (f) Foot pressure monitoring.

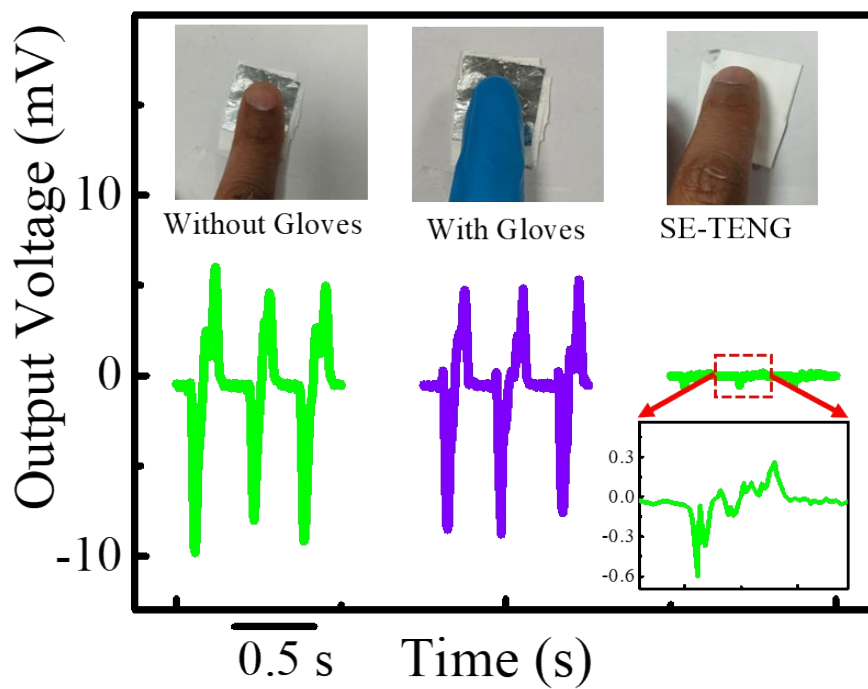


Fig. S12 Output voltage response from E-TENG upon index finger touch with and without gloves, along with single electrode E-TENG (SE-TENG) response with the same index finger touch (Inset shows the magnified view of output voltage from SE-TENG).

Table S1. Comparison of different triboelectric materials in terms of sources, sensitivity and response time.

Material used as tribo-layer	Direct source of triboelectric material	Sensitivity (V/kPa)	Response time (ms)	References
PVDF/AgNWs	Synthetic	5.84	10	1
PET/PTFE	Synthetic	45.7	< 5	2
FEP/PA	Synthetic	----	30	3
Nylon	Synthetic	7.84	20	4
yarn/conductive yarn				
Cu/PET	Synthetic	3.16	----	5
PTFE/Cellulose	Synthetic	10.184	----	6
CNC/PVDF	Synthetic	-----	48	7
PET/Cellulose	Synthetic	-----	33	8
CNC aerogel/ FEP	Synthetic	-----	68	9
PET/Ag coated conductive fiber	Synthetic	-----	80	10
This work	Natural	7.76	2.5	

Table S2. Qualitative comparison of triboelectric properties of cellulosic triboelectric materials.

Cellulose based triboelectric material	Open circuit voltage (V) (peak to peak)	Short circuit current (μA) (peak to peak)	Power density (mWm^{-2})	References
Mxene/CMC Aerogel	125	1.25	400 mWm^{-2}	11
ACA Aerogel film	104	1.52	694 mWm^{-2}	12
CN/GO Aerogel	100	12	413.2 mWm^{-2}	13
BC/HEC Aerogel	25	1	7.91 mWm^{-2}	14
TOCN Aerogel	104	8.3	156 mWm^{-2}	15
CNF/PI Aerogel	60.6	7.7	2330 mWm^{-2}	16
CNF/PANI Aerogel	125	12.5	1850 mWm^{-2}	17
CNF/PVA Aerogel	60	6	265 mWm^{-2}	18
Cellulose Aerogel	65	1.86	127 mWm^{-2}	19
CNC Aerogel	132	4.3	-	20
SPCA and NC film	152	10.8	6800 mWm^{-2}	This work

Table S3. Comparison of present work with reported electret-assisted TENGs, cellulose TENGs.

Category	Active Triboelectric materials	Voc/Isc/ Power density	Stability/ Durability	All-cellulose pair?	Reference
Fluoropolymer electret-TENG	L1: PTFE/PDMS L2: AgNWs-coated electrode	275 V 9.5 μ A 0.80 W m ⁻²	8000 Cycles	No	21
Fluoropolymer electret-TENG	L1: FEP films L2: Polyamide (PA) film/nylon	240 V 0.7 μ A 0.15 W·m ⁻²	1720 Cycles	No	22
Polymer triboelectret	L1: Sulfonic acid-grafted cellulose L2: FEP	250 V 30 μ A -	-	No	23
Cellulose TENG	L1: BC/HEC hybrid cellulose aerogel L2: PVDF	25 V 1 μ A 0.007 W m ⁻²	6000 cycles	No	24
Cellulose TENG (synthetic modification)	L1: Fluorinated cellulose aerogel/cellulose acetate nanofibers L2: FEP	~70 V 6 μ A 0.265 W m ⁻²	6000 s	No	18
Cellulose TENG	All-cellulose L1: SPCA L2: NC	152 V 10.8 μA 6.8 W m⁻²	3×3000 cycles, 90 days (tested)	Yes	This work (E-TENG)

Notes: L: Triboelectric layer surface; BC = bacterial cellulose; HEC = hydroxyethyl cellulose; PVDF = Polyvinylidene fluoride; FEP = Fluorinated Ethylene Propylene; SPCA = stearyl-modified PVA-bonded cellulose aerogel; NC = nitro-cellulose; CNF = cellulose nanofiber.

References

- 1 H. Hu, J. Song, Y. Zhong, J. Cao, L. Han, Z. Zhang, G. Cheng and J. Ding, *ACS Sens.*, 2024, **9**, 2907–2914.
- 2 K. Meng, J. Chen, X. Li, Y. Wu, W. Fan, Z. Zhou, Q. He, X. Wang, X. Fan, Y. Zhang, J. Yang and Z. L. Wang, *Adv. Funct. Mater.*, 2019, **29**, 1806388.
- 3 L. Xu, Z. Zhang, F. Gao, X. Zhao, X. Xun, Z. Kang, Q. Liao and Y. Zhang, *Nano Energy*, 2021, **81**, 105614.
- 4 W. Fan, Q. He, K. Meng, X. Tan, Z. Zhou, G. Zhang, J. Yang and Z. L. Wang, *Sci. Adv.*, 2020, **6**, eaay2840.
- 5 G. Min, A. Singh Dahiya, D. M. Mulvihill and R. Dahiya, *FLEPS 2021 - IEEE International Conference on Flexible and Printable Sensors and Systems 2021*.
- 6 L. Zhang, Y. Liao, Y. C. Wang, S. Zhang, W. Yang, X. Pan and Z. L. Wang, *Adv. Funct. Mater.*, 2020, **30**, 2001763.
- 7 Z. Niu, Q. Wang, J. Lu, Y. Hu, J. Huang, W. Zhao, Y. Liu, Y. Z. Long and G. Han, *Small*, 2024, **20**, 2307810.
- 8 B. Luo, C. Cai, T. Liu, X. Meng, X. Zhuang, Y. Liu, C. Gao, M. Chi, S. Zhang, J. Wang, Y. Bai, S. Wang and S. Nie, *Adv. Funct. Mater.*, 2023, **33**, 2306810.
- 9 C. Cai, T. Liu, X. Meng, B. Luo, M. Chi, J. Wang, Y. Liu, S. Zhang, C. Gao, Y. Bai, S. Wang and S. Nie, *ACS Nano*, 2025, **19**, 396.
- 10 Z. Lin, J. Yang, X. Li, Y. Wu, W. Wei, J. Liu, J. Chen and J. Yang, *Adv. Funct. Mater.*, 2018, **28**, 1704112.
- 11 Y. Cheng, W. Zhu, X. Lu and C. Wang, *Nano Energy*, 2022, **98**, 107229.
- 12 J. Zheng, T. Hang, Z. Li, W. He, S. Jiang, X. Li, Y. Chen and Z. Wu, *Chemical Engineering Journal*, 2023, **471**, 144548.
- 13 F. Wang, S. Wang, Y. Liu, S. Ouyang, D. Sun, X. Yang, J. Li, Z. Wu, J. Qian, Z. Zhao, L. Wang, C. Jia and S. Ma, *Nano Lett.*, 2024, **24**, 2861.
- 14 C. Luo, H. Ma, H. Yu, Y. Zhang, Y. Shao, B. Yin, K. Ke, L. Zhou, K. Zhang and M. B. Yang, *ACS Sustain. Chem. Eng.*, 2023, **11**, 9424.
- 15 Y. Song, J. Bao, Y. Hu, M. Xu, Z. Yang, Y. Liu, Q. Yang, C. Xiong and Z. Shi, *Nano Energy*, 2022, **103**, 107832.

- 16 Q. Zheng, L. Fang, H. Guo, K. Yang, Z. Cai, M. Ann, B. Meador, S. Gong, Q. Zheng, L. Fang, K. Yang, S. Gong, H. Guo, Z. Cai and M. A. B. Meador, *Adv. Funct. Mater.*, 2018, **28**, 1706365.
- 17 J. Zhao, W. Zhang, T. Liu, B. Luo, Y. Qin, C. Gao, J. Yuan, S. Wang and S. Nie, *Adv. Funct. Mater.*, 2024, **34**, 2400476.
- 18 B. Luo, C. Cai, T. Liu, X. Meng, X. Zhuang, Y. Liu, C. Gao, M. Chi, S. Zhang, J. Wang, Y. Bai, S. Wang and S. Nie, *Adv. Funct. Mater.*, 2023, **33**, 2306810.
- 19 L. Zhang, Y. Liao, Y.-C. Wang, S. Zhang, W. Yang, X. Pan, Z. Lin Wang, L. Zhang, S. Zhang, Z. L. Wang, W. Yang, Y. Liao, X. Pan and Y. Wang, *Adv. Funct. Mater.*, 2020, **30**, 2001763.
- 20 C. Cai, T. Liu, X. Meng, B. Luo, M. Chi, J. Wang, Y. Liu, S. Zhang, C. Gao, Y. Bai, S. Wang and S. Nie, *ACS Nano*, 2025, **19**, 396.
- 21 Z. Bin Li, H. Y. Li, Y. J. Fan, L. Liu, Y. H. Chen, C. Zhang and G. Zhu, *ACS Appl. Mater. Interfaces*, 2019, **11**, 20370.
- 22 P. Zhou, W. Li, J. Lan and T. Zhu, *Nat. Commun.*, 2022, **13**, 3827-.
- 23 F. Wang, Y. Hu, C. Jia, S. Wang, H. Wang, Y. Liu, S. Ouyang, S. Zhang, S. Ma, Z. Wu and L. Wang, *Nano Lett.*, 2025, **25**, 5582.
- 24 G. N. Ahn, J. A. Shin and S. Lee, *ACS Sustain. Chem. Eng.*, 2025, **13**, 6589.